Manuscript Details

Manuscript number	JOLT_2018_1206_R1
Title	Enhancing the properties of plasmonic nanowires
Article type	Research Paper

Abstract

In this paper, we show the approach to enhance the optical properties of the plasmonic nanowires from the perspectives of both field enhancement and tunability. Two different cases have been suggested for the consideration: the first one uses hollow-core metamaterial interface, while the other involves metallic nanowire metamaterial interface. It has been outlined, that the use of nanowire metamaterial interface allows for stretching the frequency range of surface wave existence from 500 THz (600 nm) to approximately 1000 THz (300 nm). Moreover, the nanowire metamaterial interface demonstrates better field confinement.

Keywords	Metamaterials; surface plasmons
Manuscript category	Nanophotonics, Biophotonics, Medical Optics
Corresponding Author	Tatjana Gric
Corresponding Author's Institution	Vilnius Gediminas Technical University
Order of Authors	Thanos Ioannidis, Tatjana Gric, Andrei Gorodetsky, Aleksej Trofimov, Edik Rafailov
Suggested reviewers	Kofi Edee, Ortwin Hess, Theodore Simos

Submission Files Included in this PDF

File Name [File Type]

cover letter.docx [Response to Reviewers]

highlights.docx [Highlights]

Plasmonic nanowires Gric Sep8.docx [Manuscript File]

To view all the submission files, including those not included in the PDF, click on the manuscript title on your EVISE Homepage, then click 'Download zip file'.

Dear Editor,

First and foremost I express heartfelt appreciation to all reviewers on behalf of the authors of the manuscript. Thank you for the comments and suggestions to improve the paper. The responses to the reviewers comments are included below.

Reviewer 1 (changes highlighted with yellow)

In the introduction, the authors should also cite previous work on SPPs in metamaterials, specifically "Hyperbolic Polaritonic Crystals Based on Nanostructured Nanorod Metamaterials" from Wayne Dickson et al., Adv. Mat. Volume27, Issue 39, October 21, 2015, Pages 5974-5980, which considers coupling to the modes supported by such metamaterials. Additionally, SERS has gone beyond simply reaching single molecule spectroscopy: recently SERS was also used to determine the molecular orientation of single molecules. For completeness, the authors should therefore include references such as "Determining molecular orientation via single molecule SERS in a plasmonic nano-gap" from Addison R. L. Marshall et al., Nanoscale Volume 9, Issue 44, July 13, 2017, Pages 17415-17421.

Addressed in the manuscript.

The authors should also mention that epsilon_m needs to be negative for SPPs to exist. Although this is naturally happening in the case of a metal, here the authors consider a metamaterial which, depending on the geometry, can have either positive or negative effective permittivity.

Addressed in the manuscript.

Similarly, the use of epsilon_m in both the SPP dispersion at the start of the document, and later as the permittivity of the metal nanorods can lead to confusion. In the present manuscripts, the dispersion of the SPP is governed by the metamaterial's effective index as the authors later imply in equation 6.

epsilon_m is used to describe the permittivity of the metal nanowires embedded into the metamaterial.

The following sentence is unclear: "The mentioned frequency stands for as the intersection point of the effective dielectric permittivity perpendicular components attained tuning the diameter of the nanowire along with the distance between them." Since it is an important point of the paper, it needs to be rewritten for clarity.

The sentence has been rewritten and the additional reference has been provided for clarity.
Addressed in the manuscript.

The authors mention that "the "jump" point" in the dispersion for their hollow core metamaterial arises while epsilon_parallel > 0 and epsilon_perpandicular < 0: I would have liked to see a short explanation of the importance of this result in terms of hyperbolic dispersion.

It is worthwhile noting, that the "jump" point arises while $\varepsilon_{\parallel} > 0, \varepsilon_{\perp} < 0$ *providing the possibilities to increase the frequency gap region with purely imaginary β prohibiting propagation.*
Addressed in the manuscript.

The following sentence needs to be rewritten for clarity: "Consequently, the external radiation dispersion line will always exist between the light line cβ and the vertical line". I believe the authors want to highlight the constant wave vector mismatch between the light line and the SPP dispersion, but the sentence is not clear: the authors refer to the light line as cβ with β having been defined as the SPP wave vector.

Consequently, the constant wave vector mismatch between the light line and the SPP dispersion occurs.
Addressed in the manuscript.

The caption of figure 3 should specify what quantity is plotted, and where the interface is between the dielectric and the metamaterial.

All the field maps depicting the magnetic field component H_y are normalized by the highest value of the magnetic field obtained in case (c). The interface between dielectric and metamaterial corresponds to the case of x=0.
Added to the caption.

The authors should focus their discussion on the system they are presenting, and the differences it presents with respect to the standard SPP sustained at a metal-dielectric interface. A lot of the discussion presents properties of the standard SPP.

The privileges of the system under consideration have been stressed in comparison with the conventional metal-dielectric interface.

It is worthwhile noting, that the "jump" point arises while $\varepsilon_{\parallel} > 0, \varepsilon_{\perp} < 0$ providing the possibilities to increase the frequency gap region with purely imaginary β prohibiting propagation. The mentioned property does not take place in case of the conventional metal-dielectric interface.

…The increase of spacing S_L causes shift of the SPPs diagrams to the lower wavelengths. It is worthwhile noting, that it is impossible to employ the described tunability mechanisms in case of the conventional metal-dielectric interface.
Addressed in the manuscript.

More is needed on the field enhancements obtained in those systems as the authors present that aspect as a characteristic of their geometry: the authors could give numbers and compare them with values for the standard metal-dielectric SPP.

Additional figure related to the standard metal-dielectric SPP has been added (Fig. 4).

Reviewer 2

I don't see a lot of difference between Figs. 3 and 4, from published paper [J. Opt. 19, 085101 (2017)] and Figs. 2 (a-d) of submitted paper.

The main difference between mentioned figures lies in the fact that different systems have been suggested for the consideration. Thus, the interface separating two nanowire metamaterials has been considered in [J. Opt. 19, 085101 (2017)]. On the contrary, the interface separating dielectric metamaterial is studied in [Enhancing the properties of plasmonic nanowires].

It is confusing that the authors titled the Fig. 2 as "Dispersion and absorption in case….". I cannot find the absorption spectra at these plots. It is also difficult to find difference between curves at these Figs. 2 (a-d), at least need to change the scale.

Absorption spectra is plotted with the dashed lines.
The scale has been modified.

The authors determined the propagation length as a function of the real and imaginary parts of permittivity of the metal, but as parallel components this permittivity. What is mean -parallel metal's permittivity.

The parallel component of the metamaterial permittivity has been employed into the expression.

In the References: References [15] and [22] coincide

Modified.

- The use of nanowire metamaterial interface allows for stretching the frequency range of surface wave existence from 500 THz (600 nm) to approximately 1000 THz (300 nm).
- The nanowire metamaterial interface demonstrates better field confinement.
- The nanowire metamaterial supports tunable surface plasmon polaritons allowing for up to 2-fold field enhancement.
- Presented results provide an approach for effective realization of nanophotonic devices such as optical reflectarrays, SPP couplers, plasmonic absorbers

Enhancing the properties of plasmonic nanowires

THANOS IOANNIDIS[1], TATJANA GRIC[1,2]*, ANDREI GORODETSKY[3,4], ALEKSEJ TROFIMOV[1], EDIK RAFAILOV[5]

[1] *Department of Electronic Systems, Vilnius Gediminas Technical University, Vilnius, Lithuania*
[2] *Semiconductor Physics Institute, Center for Physical Sciences and Technology, Vilnius, Lithuania*
[3] *ITMO University, St. Petersburg 197101, Russia*
[4] *Department of Chemistry, Imperial College London, London, SW7 2AZ, UK*
[5] *Aston Institute of Photonic Technologies, Aston University, Birmingham B4 7ET, UK*
**tatjana.gric@vgtu.lt*

Abstract: In this paper, we show the approach to enhance the optical properties of the plasmonic nanowires from the perspectives of both field enhancement and tunability. Two different cases have been suggested for the consideration: the first one uses hollow-core metamaterial interface, while the other involves metallic nanowire metamaterial interface. It has been outlined, that the use of nanowire metamaterial interface allows for stretching the frequency range of surface wave existence from 500 THz (600 nm) to approximately 1000 THz (300 nm). Moreover, the nanowire metamaterial interface demonstrates better field confinement.

OCIS codes: (160.3918) Metamaterials; (240.6680) Surface plasmons; Nanowires.

1. Introduction

Herein, we deal with the exceptional features of surface plasmon polaritons (SPPs) providing a fertile ground for plasmonics research. It is worthwhile noting, that the former phenomenon appears on the metal interface due to strong field localization. The strong level of interaction between light and free electrons in metals [1, 2] causes arise of quasiparticles, called SPPs. SPPs act as a surface wave propagating along the boundary between a metal and a dielectric while exponentially decaying into both the dielectric and metal. The dispersion relation of SPPs at a dielectric-metal boundary can be derived from Maxwell's equations with appropriate boundary conditions. Denoting the dielectric constant of the metal and the dielectric material as ε_m and ε_d, correspondingly, the dispersion equation of SPPs is expressed as

$$\beta = \frac{\omega}{c}\sqrt{\frac{\varepsilon_m \varepsilon_d}{\varepsilon_m + \varepsilon_d}} \tag{1}$$

where ω is the angular frequency of the SPP modes, c is the speed of light, and β is the wave constant of SPPs along the propagation direction. It is worthwhile noting, that the localized SPPs are dramatically influenced by the material properties along with the size and shape of the metallic nanostructures (Fig. 1a). Doing so, it is possible to achieve an efficient coupling. It should be mentioned that the exceptional properties of SPPs, such as, subwavelength confinement and strong field enhancement give rise to a wide range of innovative applications [3-7]. Moreover, propagation of SPPs in metamaterials is a hot topic either. Coupling to the modes supported by the metamaterials has been covered in [8] opening the wide avenues for the innovative aspects. For example, owing to the excitation of SPPs, resolution of the so-called "superlens" has reached as high as 30 nm [9]. The former opens the wide avenues for optical microscopy in terms of overcoming the diffraction limit. Alternatively, the resolution can be even higher in plasmonics-assisted spectroscopy, such as surface-enhanced Raman spectroscopy (SERS). The Raman signal can be considerably amplified by SERS approach. Doing so, the vibrational information of single molecules can be probed and recorded [10-12]

by employing the strong local field enhancement of plasmonic composites and the chemical mechanism including charge transfer between the species and the metal surface. Additionally, SERS has gone beyond simply reaching single molecule spectroscopy: recently SERS was also used to determine the molecular orientation of single molecules [13]. Tip-enhanced Raman spectroscopy (TERS) may stand for the further resolution improvement. Based on the study on TERS-based spectral imaging with extraordinary sub-molecular spatial resolution, one can definitely resolve the inner structure and surface configuration of a single molecule [14]. Moreover, it is worthwhile noting, that plasmonic nanoantennas give a tremendous rise to the enhancement of THz generation [15, 16].

2. Basic model

Fig. 1 displays the geometry of the nanowire structure. Metal wires with permittivity ε_m are implanted in a dielectric host material with permittivity $\varepsilon_d = 2.4$.

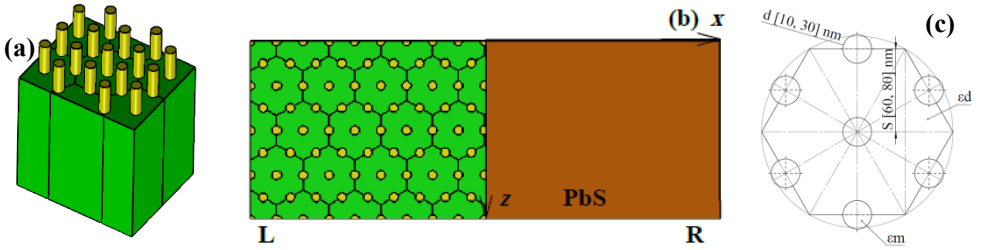

Fig. 1. Schematic view of nanowire structure (a); a view of a boundary of a nanowire composite (b); metamaterial unit cell (c)

The effective permittivities of the nanowire metamaterial are evaluated based on the effective medium approximation as follows [17]:

$$\varepsilon_{\perp}^{L} = \varepsilon_d^{L}\left[\frac{\varepsilon_m^{L}\left(1+\rho^{L}\right)+\varepsilon_d^{L}\left(1-\rho^{L}\right)}{\varepsilon_m^{L}\left(1-\rho^{L}\right)+\varepsilon_d^{L}\left(1+\rho^{L}\right)}\right] \tag{2}$$

$$\varepsilon_{\parallel}^{L} = \varepsilon_m^{L}\rho^{L}+\varepsilon_d^{L}\left(1-\rho^{L}\right) \tag{3}$$

Here, subindices L and R refer to the left and right layer, correspondingly, and ρ is the metal filling factor which is computed as:

$$\rho = \frac{nanowire\ \ area}{unit\ cell\ \ area} \tag{4}$$

It is worthwhile mentioning, that metamaterial permittivity $\varepsilon_{\parallel}^{L}$ should be negative for SPP to exist. Aiming to investigate the features of SPPs, a Drude model is used to describe the metal. Doing so, the permittivity of silver is expressed as $\varepsilon_m(\omega) = \varepsilon_\infty - \frac{\omega_p^2}{\omega^2 + i\delta\omega}$. Fitting this permittivity function to a particular frequency range of bulk material [18] allows obtaining the parameters of interest. It is found [19] that a reasonable fit might be provided for silver, if the utilized values are as follows $\varepsilon_\infty = 5$, $\omega_p = 9.5eV$, $\delta = 0.0987eV$. The metal filling ratio (ρ) is calculated utilizing the parameters, such as nanowire diameter (d) and spacing (S) and dealing with a hexagonal cell, the relation [20] might be applied as follows:

$$\rho = \frac{\pi d^2}{2\sqrt{3}S^2} \tag{5}$$

Following this assumption, a dispersion equation for the SPPs concentrated at the boundary of anisotropic media might be derived. SPP mode described by the wave vector [21]

$$\beta = k\left(\frac{\left(\varepsilon_{\parallel}^{R} - \varepsilon_{\parallel}^{L}\right)\varepsilon_{\perp}^{R}\varepsilon_{\perp}^{L}}{\varepsilon_{\perp}^{R}\varepsilon_{\parallel}^{R} - \varepsilon_{\perp}^{L}\varepsilon_{\parallel}^{L}}\right)^{1/2}, \tag{6}$$

with k being the wavenumber and β is the component of the wavevector parallel to the boundary is obtained after dealing with the tangential components of the electric and magnetic fields.
It is worthwhile noting that Eq. (6) is valid only under the condition of surface confinement, which can be presented in the following form:

$$\begin{cases}\left(k^2 - \beta^2 / \varepsilon_{\parallel}^{L}\right)\varepsilon_{\perp}^{L} < 0 \\ \left(k^2 - \beta^2 / \varepsilon_{\parallel}^{R}\right)\varepsilon_{\perp}^{R} < 0\end{cases}. \tag{7}$$

3. Simulation results and discussions

Figure 2 displays the dispersion relation (Eq. 6) utilizing the complex experimental values of permittivity. Due to the metal being not treated as lossless, β is complex. Thus, a finite propagation length of surface plasmons phenomenon is caused. At this point, the divergence of the wave vector is not observed. On the contrary, it bends backwards filling the region called plasmon bandgap and connects to the Brewster mode. The range of anomalous dispersion is called quasi-bound mode [22]. One may consider how the SPP dispersion relation departs from the light line, resembling the behavior of SPPs propagating along metal at optical frequencies (see Fig. 2). Doing so, the TM dispersion diagram for SPP modes supported by a nanowire metamaterial are shown in Fig. 2. Herein, we analyze two different cases. The light line is asymptotically approached by the SPP dispersion curves at the long wavelength due to the fact that the EM is not affected by the fine periodic structure. Though, the highly localized surface bound modes are engineered along the corrugated system if the frequency increases.

A. Interface of the nanowire metamaterial and dielectric

First, surface modes at the boundary of the nanowire metamaterial and dielectric are studied. Fig. 2 displays the dispersion diagrams of the surface modes along with the absorption graphs. In the first case (Fig. 2) the spacing is fixed, i. e. S_L=60 nm and the pore diameter is varying, i. e. d_L=10 nm, 20 nm, 30 nm. To the best of our knowledge, altering either metal or dielectric drastically affects the dispersion diagrams [23]. Herein, the impact of the spacing of the metamaterial L on the SPPs is studied. Doing so, the spacing varies from 60 to 80 nm. The influence of the spacing parameter on the surface modes dispersion characteristics is displayed in Figure 2. The increase of spacing S_L causes shift of the SPPs diagrams to the lower wavelengths. It is worthwhile noting, that it is impossible to employ the described tunability mechanisms in case of the conventional metal-dielectric interface.

B. Interface of the hollow-core metamaterial and dielectric

The hollow-core metamaterial is introduced by replacing the metal nanowires with the air holes. On the other hand, metal, i. e. Ag is used as the host material. The influence of the nanowire

geometry on the dispersion diagrams in case of the hollow-core metamaterial is studied in Fig. 2. Moreover, the influence of the distance between nanowires in the structure within different frequencies is presented in Fig. 2. It is worthwhile noting, that anomalous features of the dispersion diagrams can be observed near the frequency 10^{15} Hz in Fig. 2. The mentioned frequency is particular due to the fact that it serves as the intersection point of the effective dielectric permittivity perpendicular components obtained varying the diameter of the nanowires as well as the distance between them [17]. It is worthwhile noting, that the "jump" point arises while $\varepsilon_{\|} > 0, \varepsilon_{\perp} < 0$ [17] providing the possibilities to increase the frequency gap region with purely imaginary β prohibiting propagation. The mentioned property does not take place in case of the conventional metal-dielectric interface.

In Figs. 2 the frequency range for surface Bloch wave is narrow. Though, it is possible to extend it by dealing with the case of the nanowire metamaterial (Case A). Furthermore, the impact of the nanowire diameter on the dispersion curves (see Fig. 2) is discussed. It is found that both the upper and the lower limits shift to the higher frequencies as d is decreased. Though the movement of the lower limit is quicker than that of the upper one. Doing so, the broader frequency range for surface wave existence arises. This is consistent with the effect of d on the frequency range of negative $\varepsilon_{\|}$. One can also broaden the frequency range of surface Bloch waves by tuning the distance S [17]. A wide spectrum of possibilities to engineer the SPP at the near-infrared frequencies is provided due to the impact of the diameter and distance on the frequency range of surface wave existence.

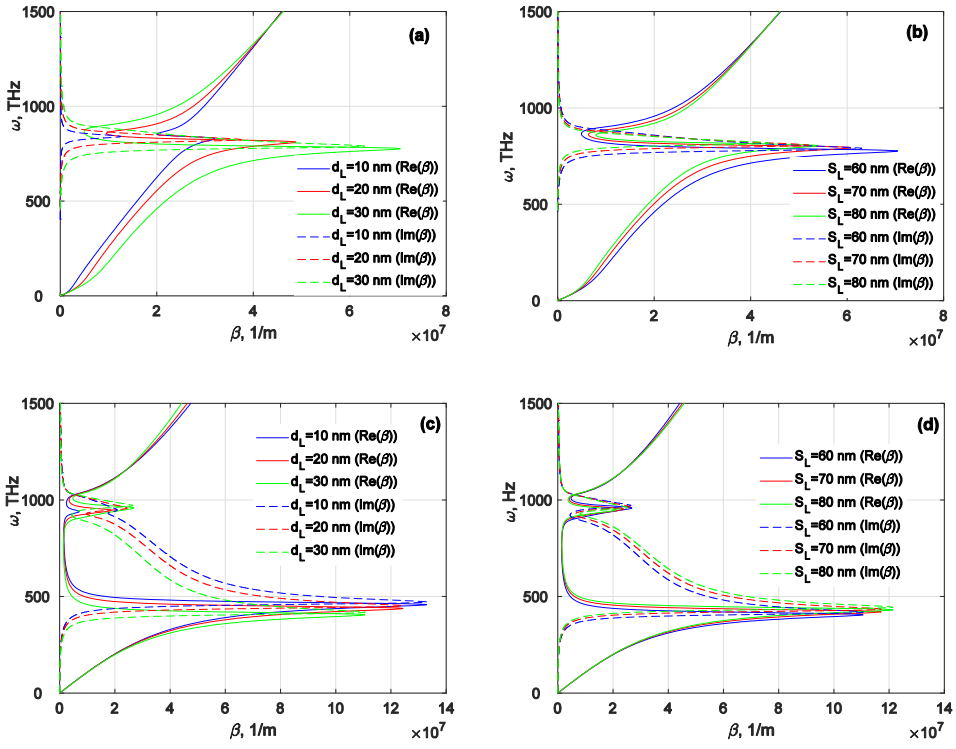

Fig 2. Dispersion and absorption in case of nanowire metamaterial interface. S_L=60 nm (a), d_L=30 nm (b). Dispersion and absorption in case of hollow-core metamaterial interface. S_L=60 nm (c), d_L=30 nm (d).

Figures 2 serve as a perfect evidence that at a given frequency free-space wavenumber k_0 is smaller than β, or that the wavelength λ_0 is longer than the SPP wavelength λ_{SPP} in the free space at the same frequency. Doing so, the slow wave effect is obtained. Hence, a mismatch in the phase of the free-space waves and SPPs takes place. Consequently, a coupler is needed, as in periodic leaky-wave antennas [24]. One may sometimes relate the concept of SPPs to Sommerfeld-Zenneck surface waves [25]. The former are known to occur at microwave frequencies.

It is noted that the wave vector β in the dispersion relation (Figs. 2) is a two-dimensional wave vector in the plane of the surface. Consequently, the constant wave vector mismatch between the light line and the SPP dispersion occurs. The described phenomenon takes place if the surface is hit by the light in an arbitrary direction. Thus, the surface plasmon polariton line will not be intersected. It means, that surface plasmons cannot be excited by light incident on an ideal surface. Nevertheless, two mechanisms, i. e. surface roughness or gratings [26], and attenuated total reflection (ATR) [27, 28] allow for the external radiation to be coupled to SPPs.

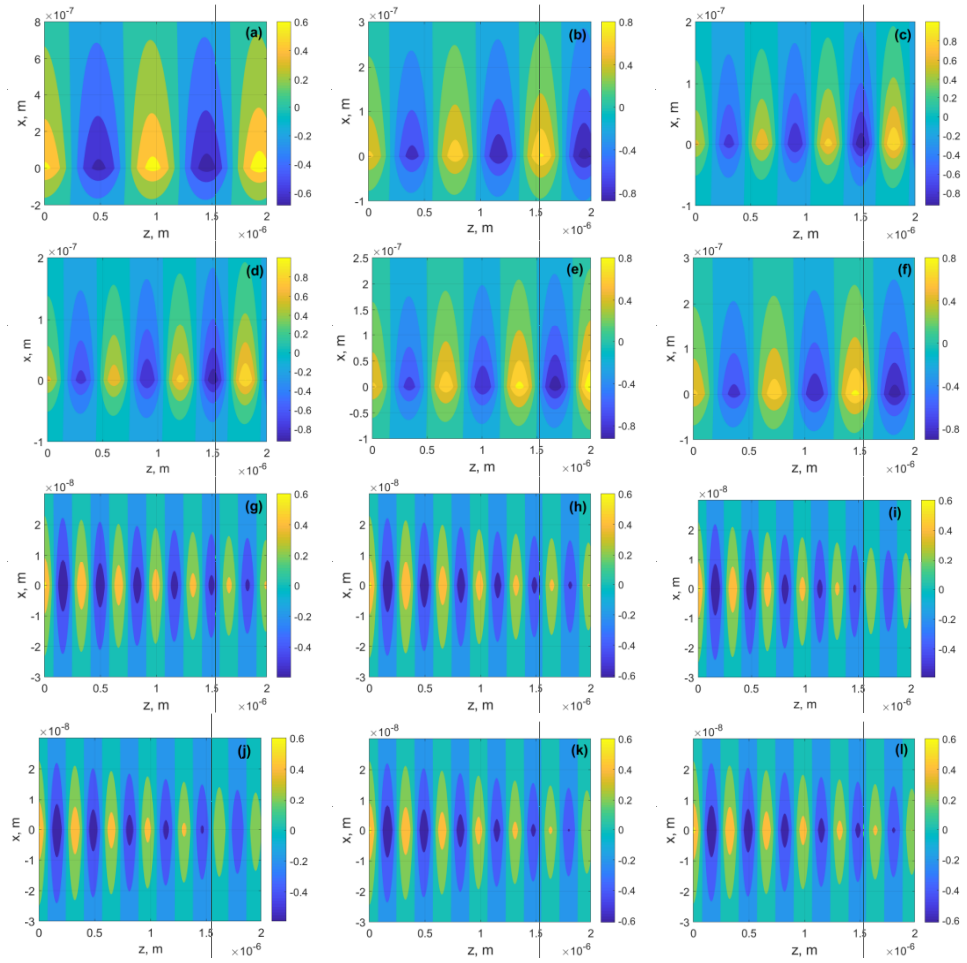

Fig. 3. A view of SPPs at a nanowire metamaterial-dielectric interface: (a) d_L=10 nm, (b) d_L=20 nm, (c) d_L=30 nm. S_L=60 nm. (d) S_L=60 nm, (e) S_L=70 nm, (f) S_L=80 nm. d_L=30 nm. A view of SPPs at a hollow-core metamaterial-dielectric interface: (g) d_L=10 nm, (h) d_L=20 nm, (i) d_L=30 nm. S_L=60 nm. (j) S_L=60 nm, (k) S_L=70 nm, (l) S_L=80 nm. d_L=30 nm, λ=1.55 μm. All the field maps depicting the magnetic field component H_y are normalized by the highest value of the

magnetic field obtained in case (c). The interface between dielectric and metamaterial corresponds to the case of x=0.

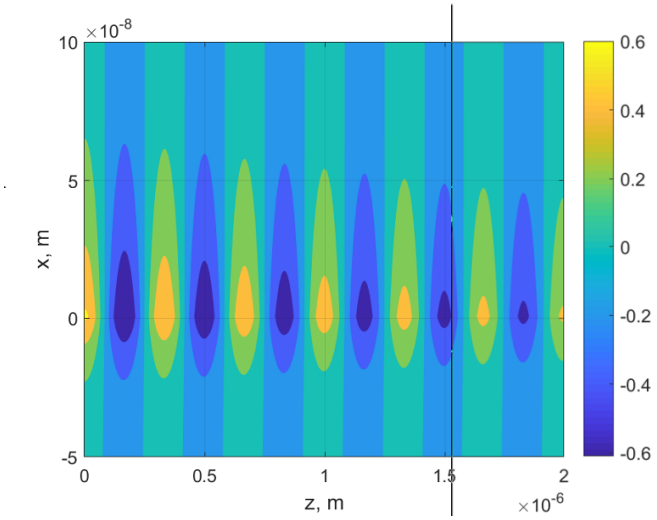

Fig. 4. A view of SPP at a metal-dielectric interface. The field map depicting the magnetic field component H_y is normalized by the highest value of the magnetic field obtained in case (Fig. 3c). The interface between dielectric and metal corresponds to the case of x=0.

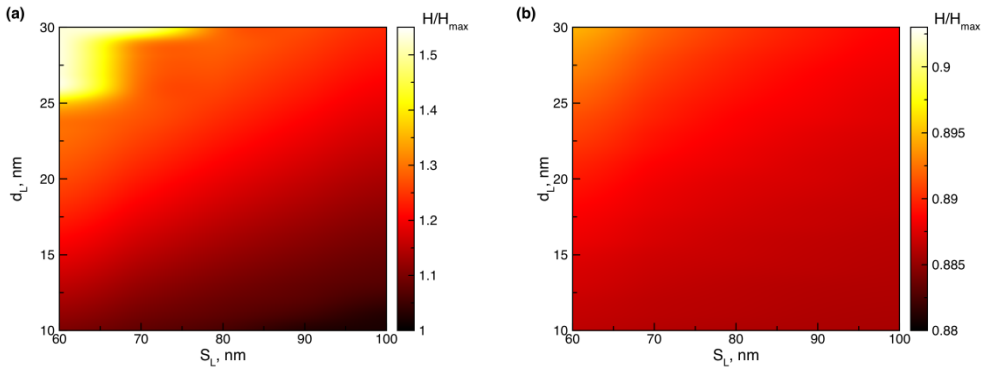

Fig. 5. Dependence of the normalized magnetic field upon the distance d_L of the metamaterial unit cell for a nanowire (a) and hollow-core (b) metamaterial cases.

Aiming to study the possible approaches to coupling, we consider the spatial extension of the electromagnetic field associated with the SPP (see figures 3). One may obtain the field distribution of each guide mode by the analytical approach at each eigenfrequency. Figures 3 (g, h, i, j k, l) show the snapshot of the fields of the modes presented in Fig. 2. It is worthwhile noting, that the field maps have been obtained, when ω=193 THz (λ=1.55 μm). The chosen frequency corresponds to the propagation regimes for both cases under consideration (Fig. 2). Moreover, figures 3(g-l), 4 correspond to hollow-metamaterial case and metal-dielectric interface correspondingly. The former clearly demonstrates the weaker field confinement in comparison to the nanowire case.

For the sake of simplicity, the dispersion equation of SPP modes has been sketched schematically in Figures 2. Herein, some properties of SPP mode on the flat metamaterial/dielectric boundary are summarized as follows. (1) The SPP mode is an

electromagnetic wave coupled with the surface electron-density oscillations. The magnetic field of the mode is perpendicular to the propagation direction (TM mode) and parallel to the metal surface. As an alternative, the electric field has both the normal ($E_\perp$) and tangent ($E_\parallel$) components. On the dielectric side, $E_\perp / E_\parallel = \sqrt{\varepsilon_\parallel^L / \varepsilon_d}$; on the metamaterial side, $E_\perp / E_\parallel = -\sqrt{\varepsilon_d / \varepsilon_\parallel^L}$. Consequently, the electric field inside the metamaterial is tangent and the electrons move back and forth in the propagation direction. Then, a longitudinal electron-density wave is formed if the frequency is well below the plasma frequency. (2) The SPP mode can propagate along the metal surface with a larger propagation constant ($\beta > k_0\sqrt{\varepsilon_d}$). The former leads to a smaller propagation velocity of the electromagnetic wave on top of to the reduced wavelength. It is worthwhile noting, that the propagation length of SPP mode is finite taking the metal absorption into account. It is shown by the detailed calculation that the energy propagation length can be expressed as $L_{spp} \approx \varepsilon_\parallel'^2 / k_0 \varepsilon_\parallel'' \varepsilon_d^{3/2}$, where $\varepsilon_\parallel'$ and $\varepsilon_\parallel''$ are the real and imaginary parts of permittivity of the metal, respectively. In the visible and near-infrared region, L_{spp} is from several to hundreds of micrometers. (3) The SPP mode is evanescent on either side of the boundary because of the larger propagation constant. On the dielectric side, the decaying length of the field is $\delta_d \approx \sqrt{|\varepsilon_\parallel'|} / k_0 \varepsilon_d$; on the other side, the decaying length is $\delta_m \approx 1 / k_0 \sqrt{|\varepsilon_\parallel'|}$. This suggests that the wave is strongly confined to the metamaterial surface, which is just desired in practice. Moreover, it is noted that a strong level of enhancement of fields near the interface can also be obtained.

To get a deeper insight into the properties of SPPs, we have sketched the dependence of the normalized magnetic field upon the distance d_L in the metamaterial unit cell. It is worthwhile noting, that the higher field values are obtained in the case of the nanowire metamaterial.

4. Conclusion

It has been shown that usage of nanowire metamaterial interface allows the increase of the frequency range of surface wave existence from 500 THz (600 nm) to approximately 1000 THz (300 nm). Moreover, they demonstrated the ability to support tunable SPPs and up to 2-fold field enhancement. We believe that presented results provide an approach for effective realization of nanophotonic devices such as optical reflectarrays, SPP couplers, plasmonic absorbers. Plasmonic nanowires have given rise for integrated optics and nanodevices for sensing applications. Such devices could lead to efficient and delicate control on nanoscale light-matter interactions for advanced applications in photonics after further explorations on dielectric materials, structure topologies, and fabrication technologies.

References and links

1. H. Raether, Surface plasmons. (Springer-Verlag Berlin, 1988).
2. S. A. Maier, Plasmonics: fundamentals and applications. (Springer Science+Business Media, 2007).
3. J. N. Anker, W. Paige Hall, O. Lyandres, N. C. Shah, J. Zhao, R. P. Van Duyne, "Biosensing with plasmonic nanosensors," Nature Materials **7**, 442-453 (2008).
4. X. Zhang, Z. Liu, "Superlenses to overcome the diffraction limit," Nature Materials **7**, 435-441 (2008).
5. H. A. Atwater, A. Polman, "Plasmonics for improved photovoltaic devices," Nature Materials **9**, 205-213 (2010).
6. W. Srituravanich, N. Fang, C. Sun, Q. Luo, X. Zhang, "Plasmonic nanolithography," Nano Letters **4**, 1085-1088 (2004).
7. D. K. Gramotnev, S. I. Bozhevolnyi, "Plasmonics beyond the diffraction limit," Nature Photonics **4**, 83-91 (2010).
8. W. Dickson, S. Beckett, C. McClatchey, A. Murphy, D. O'Connor, G. A. Wurtz, R. Pollard, A. V. Zayats, "Hyperbolic polaritonic crystals based on nanostructured nanorod metamaterials," Advanced Materials **27**(39), 5974-5980 (2015).
9. P. Chaturvedi, W. Wu, V. J. Logeeswaran, Z. Yu, M. S. Islam, S. Y. Wang, R. Stanley Williams, N. X. Fang, "A smooth optical superlens," Applied Physics Letters **96**, 043102 (2010).

10. S. Nie, S. R. Emory, "Probing single molecules and single nanoparticles by surface-enhanced Raman scattering," Science **275**, 1102-1106 (1997).
11. K. Kneipp, Y. Wang, H. Kneipp, L. T. Perelman, I. Itzkan, R. R. Dasari, M. S. Feld, "Single molecule detection using surface-enhanced Raman scattering (SERS)," Physical Review Letters **78**, 1667 (1997).
12. A. Campion, P. Kambhampati, "Surface-enhanced Raman scattering," Chemical Society Reviews **27**, 241-250 (1998).
13. A. R. L. Marshall, J. Stokes, F. N. Viscomi, J. E. Proctor, J. Gierschner, J.-S. G. Bouillard, A. M. Adawi, "Determining molecular orientation via single molecule SERS in a plasmonic nano-gap," Nanoscale **44** (2017).
14. R. Zhang, Y. Zhang, Z. C. Dong, S. Jiang, C. Zhang, L. G. Chen, L. Zhang, Y. Liao, J. Aizpurua, Y. Luo, J. L. Yang, J. G. Hou, "Chemical mapping of a single molecule by plasmon-enhanced Raman scattering," Nature **498**, 82-86 (2013).
15. S. Lepeshov, A. Gorodetsky, A. Krasnok, E.U. Rafailov, P. Belov, "Enhancement of terahertz photoconductive antenna operation by optical nanoantennas," Laser & Photonics Reviews **11**(1), 1600199 (2017).
16. S. Lepeshov, A. Gorodetsky, A. Krasnok, N. Toropov, T.A. Vartanyan, P. Belov, A. Alú, E.U. Rafailov, "Boosting Terahertz Photoconductive Antenna Performance with Optimised Plasmonic Nanostructures," Scientific Reports **8**(1), 6624 (2018).
17. T. Gric, O. Hess, "Surface plasmon polaritons at the interface of two nanowire metamaterials," Journal of Optics **19**(8), 085101 (2017).
18. P. B. Johnson, R. W. Christy, "Optical constants of the noble metals," Phys. Rev. B **6**, 4370 (1972).
19. C. Oubre, P. Nordlander, "Finite-difference time-domain studies of the optical properties of nanoshell dimers," J. Phys. Chem. B **109**(20), 10042-10051 (2005).
20. R. Starko-Bowes, J. Atkinson, W. Newman, H. Hu, T. Kallos, G. Palikaras, R. Fedosejevs, S. Pramanik, Z. Jacob, "Optical characterization of Epsilon Near Zero, Epsilon Near Pole and hyperbolic response in nanowire metamaterials," J. Opt. Soc. Am. B **32**(10), 2074-2080 (2015).
21. I. Iorsh, A. Orlov, P. Belov, Y. Kivshar, "Interface modes in nanostructured metal-dielectric metamaterials," Appl. Phys. Lett. **99**, 151914 (2011).
22. J. A. Dionne, L. A. Sweatlock, H. A. Atwater, A. Polman, "Planar metal plasmon waveguides: frequency-dependent dispersion, propagation, localization, and loss beyond the free electron model," Physical Review B **72**(7), 075405 (2005).
23. T. Gric, "Surface-Plasmon-Polaritons at the interface of nanostructured metamaterials," Pr. Electromagn. Res. M **46**, 165–172 (2016).
24. D. R. Jackson, C. Caloz, T. Itoh, "Leaky-wave antennas," Proc. IEEE **100**(7), 2194-2206 (2012).
25. A. Ishimaru, J. Dexter Rockway, Y. Kuga, S.-W. Lee, "Sommerfield and Zenneck wave propagation for a finitely conducting one-dimensional rough surface," IEEE Transactions on Antennas and Propagation **48**(9), 1475-1484 (2000).
26. Y.-Y. Teng, E. A. Stern, "Plasma Radiation from Metal Grating Surfaces," Phys. Rev. Lett. **19**, 511 (1967).
27. A. Otto, "Excitation of nonradiative surface plasma waves in silver by the method of frustrated total reflection," Z. Phys. **216**, 398 (1968).
28. E. Kretschmann, H. Raether, "Radiative decay of non radiative surface plasmons excited by light," Z. Naturf. A **23**, 2135 (1968).